Computational study of the C-H···H-C contacts in Valine-methane complexes.

Neetha Mohan[1†], Adrian Varela-Alvarez[†1,2], Ramana Chintalapalle[2], and Suman Sirimulla[1,2]*.

AUTHOR ADDRESS (Word Style "BC_Author_Address").

1. Department of Pharmaceutical Sciences, School of Pharmacy, The University of Texas at El Paso.
2. Center for Advanced Materials Research (CMR), University of Texas at El Paso, El Paso, Texas

† represents equal contribution

KEYWORDS (Word Style "BG_Keywords"). Homopolar dihydrogen bonds, intermolecular forces, molecular recognition

ABSTRACT: A series of complexes between neutral Valine and methane that feature potential homopolar C-H···H-C contacts were located on the MP2/aug-cc-pVTZ potential energy hypersurface. In order to better estimate the strength of this contacts, the interaction energies were improve by single-point calculations at different levels of theory (MP2, CCSD(T), SAPT2, SAPT2+3) together with Dunning's basis sets (aug-cc-pVXZ; X=T,Q,5). Topological analysis of the electron density within the QTAIM framework, NCI plots and energy decomposition within the SAPT framework were used to discuss the nature of this interactions. The complexes whose monomers only interact though C-H···H-C contacts indicate that these interactions are entirely due to dispersion forces, are not directional and are much stronger than expected (the interaction energies of the complexes range from -0.7 to -1.0 kcal/mol). This large value is remarkable considering the small size of the interacting groups herein considered (methane, and one or two Valine's methyl groups), and indicates that in biological systems, where those interactions can be very numerous in the presence of multiple aliphatic amino acids, if those interactions are not properly model, magnitudes as ligand-receptor affinities, protein-protein interaction energies and protein stabilities might be grossly misestimated. Finally, since some of the computed complexes also include stronger interactions than homopolar C-H···H-C contacts, we analyzed if the potential C-H···H-C contacts in these complexes are really contributing to stabilize the complexes or are just a geometrical artifact arising from the maximization of stronger interactions.

INTRODUCCION

Intramolecular interactions among amino acid side chains contribute significantly to the structural stability and conformational dynamics of proteins. The interplay of various canonical interactions like hydrogen bonds, salt bridges and hydrophobic interactions,[1-3] and a variety of non-canonical interactions like CH···π, OH···π, NH···π, π···π stacking, and cation···π interactions between amino acid residues[4] play an important role in protein stability. The role of hydrogen bonds (X-H···Y) in protein stability and molecular recognition have been investigated extensively by experimental investigations and theoretical predictions. There is a considerable amount of literature on dihydrogen bonding M-H···H-X, which is a particular kind of hydrogen bonding interaction between a transition metal or main-group hydride (M-H) and a protic hydrogen moiety (H-X). The potential contribution of homopolar dihydrogen bonds (C-H···H-C) to protein stability and the nature of this sort of interaction itself was overlooked until very recently. In contrary to the highly directional hydrogen bonds and dihydrogen bonds that exist between interacting groups of different polarities, C-H···H-C contacts involve hydrogen atoms of similar polarity and are expected to be weak, non-directional and resulting from induced dipole-induced dipole (dispersion) interactions. Homonuclear C-H···H-C interactions hold alkanes together in the solid state and in the lipid parts of cell membranes.

The existence, strength and nature of homopolar dihydrogen bonds has led to a stimulating debate among researchers. Pioneering theoretical calculations by Bader and coworkers using the Quantum Theory of Atoms in Molecules (QTAIM) confirmed the existence of C-H···H-C bond critical points (BCPs) and paths (BPs) in planar aromatic systems composed of fused-phenyl rings, which was associated with a stabilizing C-H···H-C bonding interaction.[5,6] On the other hand, Bikelhaupt and co-workers applied the Electron Decomposition Analysis (EDA) to planar diphenyl and concluded that the C-H···H-C bonding predicted by QTAIM does not really exist, instead describing such C-H···H-C contact as a mere (repulsive) steric interaction.[7,8] While Bader claimed that disagreement was due to the lack of theoretical rigor of the EDA method, Bikelhaupt and co-workers pointed towards a lack of "any predictive power" of QTAIM.[9,10] Hernandez-Trujillo and Matta revisited this system and analyzed the interaction of the atoms in different phenyl rings within the QTAIM framework, founding that in fact there is an attractive H···H interaction and that the rotational barrier associated to the planar conformation arises from a destabilization of the biphenyl C-C bond.[11] Likewise, Palacios and Gomez concluded that there is an H···H attractive interaction based on their analysis of the electrostatic potential.[12] Popelier and coworkers applied the interacting quantum atoms (IQA) approach (IQA) to the rotational profile of biphenyl and concluded that the observed planar barrier is indeed due to steric interactions between the hydrogen atoms, but they also found a stabilizing covalent bonding interaction between those two hydrogen, but the magnitude of this contribution is smaller compare to the steric repulsion.[13] Alvarez and coworkers confirmed the stabilizing nature of C-H···H-C contacts between saturated alkanes and polyhedranes, and showed that these kind of homonuclear dihydrogen contacts are subtle but much stronger than previously thought.[14] Recently, Cuevas and co-workers estimated the nature and magnitude of the interactions in 11 different relative orientations of methane dimer using electron density analysis and energy decomposition analysis.[15]

The van der Waals interactions between buried non-polar side chains of amino acids are expected to play a significant role in protein folding and stability, making the contribution of C-H···H-C contacts between alkyl side chains critical. The existence and nature of these subtle homopolar dihydrogen interactions and their role in the stabilization of proteins and protein-ligand interactions is greatly overlooked. Herein, we computationally study and analyze several weakly-bound complexes featuring potential C-H···H-C contacts between a nonpolar amino acid, Valine, and a nonpolar probe molecule, methane (CH_4). We expect this model system would represent a first step towards the understanding of the contribution of C-H···H-C sidechain interactions towards protein stabilization.

METHODS

Electronic structure calculations. Gas-phase geometry optimizations were performed by means of the second order Møller-Plesset perturbation theory (MP2) together with the Dunning's aug-cc-pVTZ basis set.[16-19] In order to improve our predictions of the interaction energy, single-point energy correction were computed at different levels of theory: MP2/aug-cc-pVTZ, MP2/aug-cc-pVQZ, MP2/aug-cc-pVQZ, and Coupled Cluster with connected single, double and perturbative triple contributions together with the aug-cc-pVTZ basis set (CCSD(T)/aug-cc-pVTZ).[16-19] Boys-Bernardi counterpoise (CP) method was used to computed the corresponding basis set superposition error (BSSE)-corrected values of the interaction energy.[18,20] The interaction energy was also computed using the symmetry-adapted perturbation theory (SAPT) together with the aug-cc-pVTZ basis set.[21] All calculations were performed using Psi4 1.3. [22]

Analysis of the electron density. Topological analysis of the electron density based on the quantum theory of atoms in molecules (QTAIM) as well as non-covalent index (NCI) plots were generated using Multiwfn 3.7.[5,23-25]

Visualization software. The molecular structures showcasing the geometrical parameters were built using Avogadro 1.2.0,[26] QTAIM figures were built using Multiwfn,[25] and NCI figures were built using VMD.[27]

RESULTS AND DISCUSSION

1. Geometries. Figures 1-3 collect the 26 different Valine-methane complexes that have been located on the MP2/aug-cc-pVTZ potential energy hypersurface (PES). The goal was not to exhaustively locate all the possible complexes but to find a large number of complexes that exhibit potential C-H···H-C contacts, so we can better understand the nature and energetic range of these contacts in systems of biological interest. All these complexes were characterized as real minima through a vibrational analysis with the exception two of them, **Val-Met_5b** (**Figure 2**) and **Val-Met_0c** (**Figure 3**), which exhibit one small imaginary frequency each (12i cm-1 and 15i cm-1, respectively). All our attempts to converge these two complexes to minimum structures were unsuccessful and, bearing in mind the lower absolute value of those imaginary frequencies and the fact that for each

complex there are two other analog complexes that were characterized as minima (**Val-Met_5a** and **Val-Met_5c**, and **Val-Met_0a** and **Val-Met_0b**, see **Figures 1-3**), we think that is reasonable to assume that those imaginary frequencies may arise from numerical instabilities on the frequency computation.

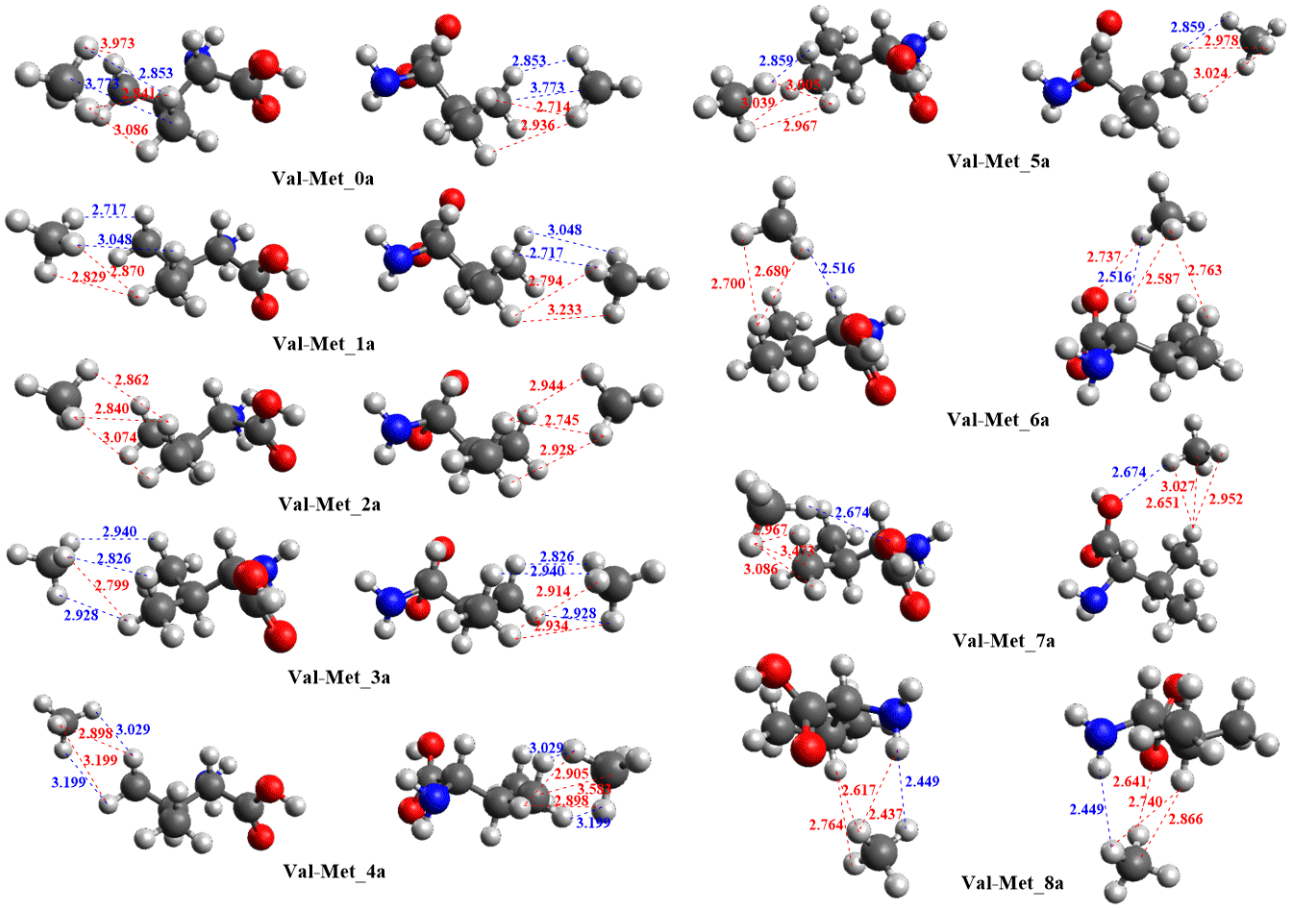

Figure 1. Valine-Methane complexes located on the MP2/aug-cc-pVTZ PES belonging to the series a. Two views of each structure are shown. Some selected intermolecular distances are given (Å). Blue values represent distances that are highlighted in both views while red values represent distances that highlighted in only one of the views.

The 26 weakly bound complexes have been divided in three different series: series a (from **Val-Met_0a** to **Val-Met_8a**, see **Figure 1**), series b (from **Val-Met_0b** to **Val-Met_8b**, see **Figure 2**) and series c (from **Val-Met_0c** to **Val-Met_8c**, see **Figure 3**). Members of each series share a similar conformation of the Valine monomer, while complexes labelled with the same number (0-8) but belonging to different series are similar to each other and differ on the Valine conformation (occasionally also on the interaction pattern between Valine and methane, precisely as a consequence of the different Valine conformations considered; please, compare for instance **Val-Met_4a** with **Val-Met_4b**, and **Val-Met_6a** with **Val-Met_6b**, collected in **Figures 1** and **2**).

While series a and c include 9 complexes, series b only includes 8 (see **Figures 1-3**) since we failed to locate structure **Val-Met_7b**. Our attempts to obtain **Val-Met_7b** generally ended up producing **Val-Met_6b** due to how easily the system picks up the C-H···H-O intermolecular interaction; that is, the barrier interconverting **Val-Met_6b** and **Val-Met_7b** may be too low, or even the C-H···H-O interaction may be strong enough to prevent the formation of a minimum resembling **Val-Met_7b** on the PES. Such C-H···H-O interaction cannot occur in the conformations Valine adopts for series a and c, and for this reason we were able to easily locate **Val-Met_7a** and **Val-Met_7c** but not their analog **Val-Met_7b**.

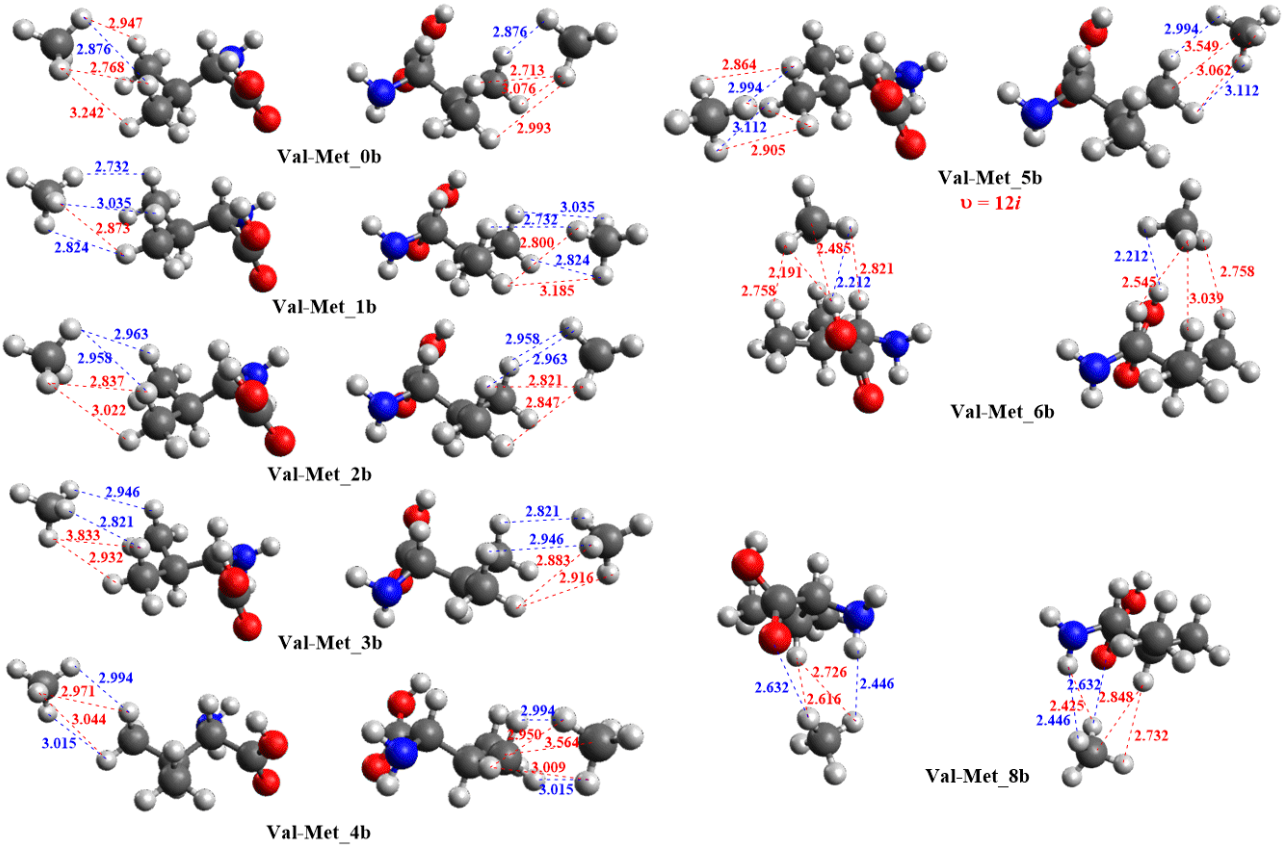

Figure 2. Valine-Methane complexes located on the MP2/aug-cc-pVTZ PES belonging to the series b. Two views of each structure are shown. Some selected intermolecular distances are given (Å). Blue values represent distances that are highlighted in both views while red values represent distances that highlighted in only one of the views. For the structures predicted to have a small imaginary frequency is value in cm^{-1} is in red right under the structure label.

Within each series, the complexes can be further divided in three subsets. Complexes from **Val-Met_0x** to **Val-Met_3x** (x = a, b, c) form a subset of structures exhibiting potential C-H···H-C contacts between the methane and both methyl groups of the Valine's sidechain. Complexes **Val-Met_4x** and **Val-Met_5x** (x = a, b, c) are alike in the sense that they only exhibit potential C-H···H-C contacts between the methane and one of the two methyl groups of the Valine's sidechain. Finally, complexes from **Val-Met_6x** to Val-**Met_8x** (x = a, b, c) can be grouped together into a subset of compounds that exhibit potential C-H···H-C contacts together with other potential stronger interactions, such as C-H···H-N contacts (see for example **Val-Met_8a** in **Figure 1**). This last subset will allow us to investigate whether C-H···H-C attractive interactions survive in the presence of stronger interaction or they get turned into steric repulsive interactions accounting for a small energy penalty to pay in order to maximize a stronger interaction.

For a given x, the geometries of the **Val-Met_0x** to **Val-Met_3x** (x = a, b, c) are only slightly different and difficult to tell apart for the untrained eye (see **Figures 1-3**). Each of them exhibits potential contacts with both methyl groups and only differ due to subtle translations and rotations of the methane respect to the Valine. That may be a consequence of the generally assumed nature of the C-H···H-C contacts: weak, additive interactions that lack the directional nature of other stronger interactions such as hydrogen bonds. In other words, the minima located seem to maximize the number of potential contacts instead of adopting geometries that maximize the strength of a few contacts. In fact, for all the **Val-Met_0x** to **Val-Met_3x** (x = a, b, c) complexes, there are always five or six intermolecular H···H distances within the 2.7-3.1 Å (arbitrary) range, which hints towards a large number of C-H···H-C contacts, being the only exception **Val-Met_0c** that exhibits just four H···H distances within that range (see **Figure 1-3**).

As mentioned before, the methane is potentially interacting with both methyl groups of the Valine sidechain in the **Val-Met_0x** to **Val-Met_3x** (x = a, b, c) structures, but that interaction is not symmetric. The distances between the methane's carbon center and the carbon centers of the Valine's methyl groups are collected in **Chart 1**. For **Val-Met_0x** to **Val-Met_2x** (x = a, b, c), r_1 distance is always longer than r_2, indicating a stronger interaction with methyl group B (see **Chart 1**). The opposite is observed for **Val-Met_3x** (x = a, b, c), indicating that in this case the interaction is stronger with the methyl group A (see **Chart 1**). In any case, the difference between those two distances is always around 0.2 Å, and it is safe to assume that for those 12 complexes the methane is interacting with both sidechains' methyl groups.

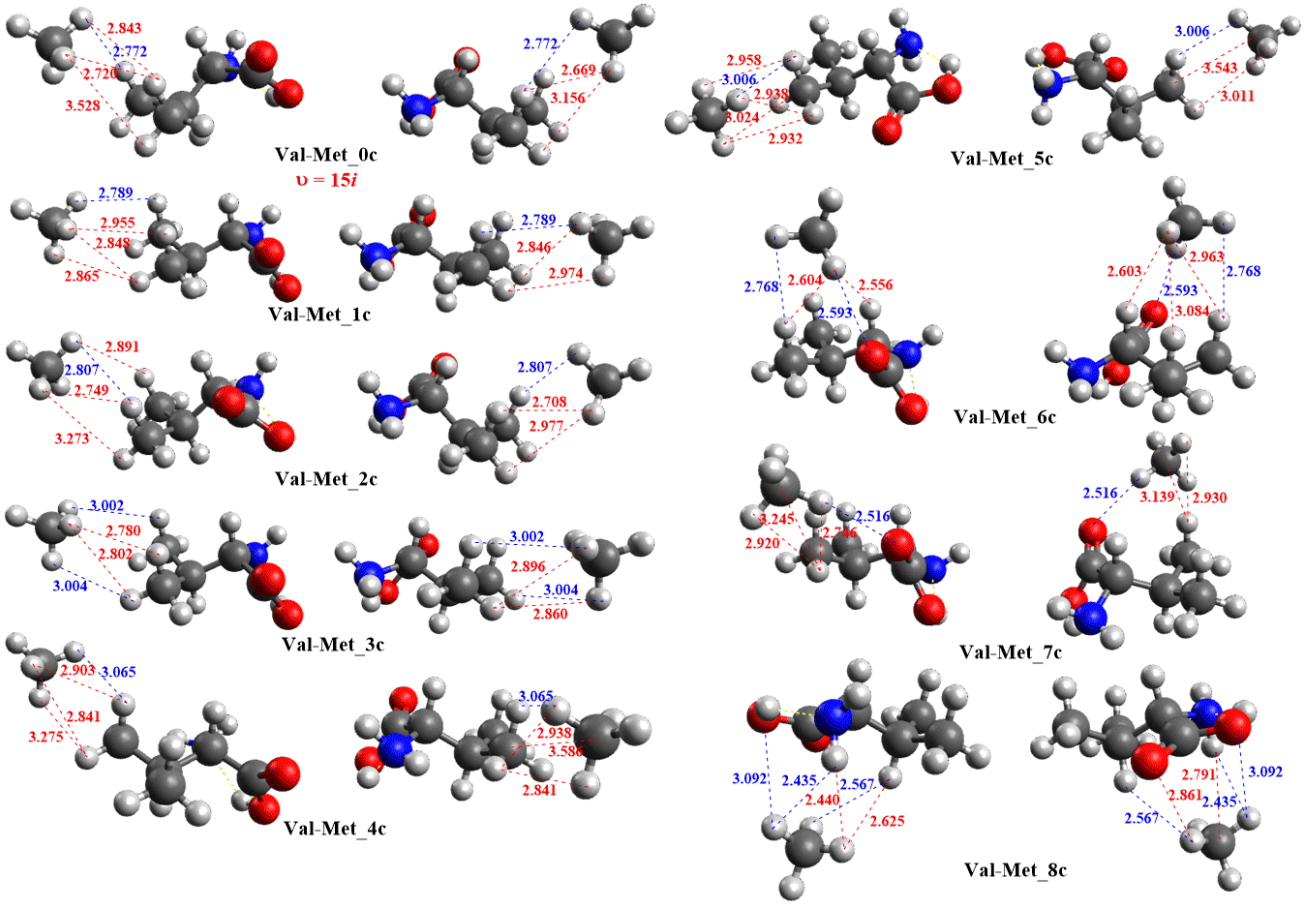

Figure 3. Valine-Methane complexes located on the MP2/aug-cc-pVTZ PES belonging to the series c. Two views of each structure are shown. Some selected intermolecular distances are given (Å). Blue values represent distances that are highlighted in both views while red values represent distances that highlighted in only one of the views. For the structures predicted to have a small imaginary frequency is value in cm^{-1} is in red right under the structure label.

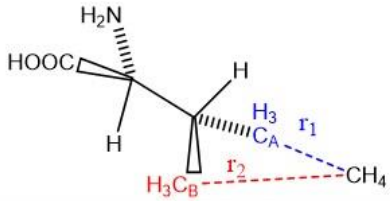

	x = a		x = b		x = c	
	r_1	r_2	r_1	r_2	r_1	r_2
Val-Met_0x	4.021	3.773	4.042	3.797	4.042	3.854
Val-Met_1x	4.026	3.789	4.024	3.779	3.970	3.799
Val-Met_2x	4.014	3.772	4.003	3.786	3.998	3.817
Val-Met_3x	3.790	3.971	3.802	3.970	3.769	3.991
Val-Met_4x	3.583	5.897	3.564	5.804	3.586	5.901
Val-Met_5x	5.755	3.552	5.832	3.549	5.777	3.543
Val-Met_6x	4.362	3.992	4.803	4.117	4.639	3.938
Val-Met_7x	5.783	3.781	-	-	5.908	3.687
Val-Met_8x	4.657	4.868	4.604	4.870	4.553	5.061

Chart 1. Carbon-carbon distances between each methyl group of the valine and the methane for the 26 complexes located.

Let us focus now on complexes **Val-Met_4x** and **Val-Met_5x** (x = a, b, c), which exhibit interactions between the Methane and only one of the Valine's methyl groups (see **Figures 1-3**). For these six structures, the methane interacts with the methyl group adopting a staggered conformation instead of an eclipsed one. We again attribute that to the fact that this C-H···H-C interactions are weak but additive, so the system prefers to maximize the number of potential contacts (up to six in the staggered conformation) instead of forming a smaller number of stronger contacts (up to three in the staggered conformation). It is also interesting to note that the C···C distance of the interacting groups is now lower than any C···C distance in the **Val-Met_nx** (n = 0-3; x = a, b, c) complexes, where the methane is interacting with two methyl groups at the same time and can afford a larger separation from each methyl in order to build more contacts with both methyl groups instead of only one (see **Figures 1-3** and **Chart 1**).

Now we focus our attention on the eight complexes that exhibit other potential and stronger interactions besides C-H···H-C contacts: **Val-Met_6x** (x = a, b, c), **Val-Met_7x** (x = a, c) and **Val-Met_8x** (x = a, b, c). Based on the geometry parameters collected in **Figures 1-3**, all of them except **Val-Met_6b** feature C-H···:O interactions. The largest H···O distance observed is 2.861 Å (**Val-Met_8c**, see **Figure 3**) while the shortest one is 2.516 Å (**Val-Met_7c**, see **Figure 3**). The three **Val-Met_8x** (x = a, b, c) complexes all exhibit potential C-H···H-N contacts whose associated distances range from

2.425 to 2.449 Å (see **Figures 1-3**). Only one complex exhibit potential C-H···H-O contacts, **Val-Met_6b** (see **Figure 2**), which exhibits two potential contacts characterized by H···H distances of 2.191 and 2.212 Å (see **Figure 2**). All these complexes also appear to build C-H···H-C contacts, although for the three **Val-Met_8x** (x = a, b, c), none of those C-H···H-C potential contacts involve the sidechain's methyl groups (see **Figures 1-3** and the C···C distance values collected in **Chart 1**). Although many of them lie within the usual 2.7-3.1 Å range, almost all of them, except for **Val-Met_7c**, exhibit examples of shorter C-H···H-C distances ranging from 2.54 to 2.65 Å (see **Figures 1-3**). It is fair to wonder whether those shorter values represent stabilizing C-H···H-C contacts or some sort of steric, repulsive interaction.

2. Interaction energies. Table 1 collects the interaction energies for the 26 complexes located on the MP2/aug-cc-pTZ PES at different levels of theory:

I. MP2/aug-cc-pVXZ (X = T, Q, 5). Second order Møller-Plesset (MP2) results computed with different Dunning's basis sets. Both, basis-set superposition error (BSSE) uncorrected and corrected results, using the counterpoise (CP) method, are included.

II. SAPTx/aug-cc-pVTZ (x = 0, 2, 2+3). Different levels of Symmetry-adapted perturbation theory (SAPT) together with a Dunning's triple-ζ basis set. There are two main advantages of using SAPT methods: this interaction energies are BSSE free due to the nature of this calculations, and the interaction energy is naturally decomposed on a series of terms with easy physical interpretation. SAPT0+D interaction energies are equivalent to Hartree-Fock (HF) interaction energies plus a dispersion correction (including the corresponding dispersion-exchange term). SAPT2 interaction energies are roughly equivalent to MP2 interaction energies. Finally, SAPT2+3 includes additional terms, and the quality of its results can be compared to MP4 interaction energies.

III. CCSD(T)/aug-cc-pVTZ. Coupled cluster with connected single-doubles excitation and perturbative triple excitations (CCSD(T)) calculations with a Dunning's triple-ζ basis set. Both uncorrected and CP-corrected results are provided.

IV. CCSD(T)/aug-cc-pVTZ+δ(aV5Z). Our highest computational level of theory includes interaction energies computed at the CCSD(T)/aug-cc-pVTZ plus a δaV5Z correction computed as the difference between the MP2/aug-cc-pV5Z and MP2/aug-cc-pVTZ energies.

There are some general patterns arising from the data collected in **Table 1**. First, the interaction energies at the MP2/aug-cc-pVTZ and CCSD(T)/aug-cc-pVTZ level of theory are rather similar. In general, MP2 overestimates its value (they tend to be smaller in absolute value) as the positive mean signed deviation (m.s.d. = 0.028 kcal/mol) reveals. That difference for each of the complexes is always smaller than 0.1 kcal/mol (in absolute value) and the mean absolute error (m.a.e.) is only 0.036 kcal/mol. Considering this small value of the m.a.e. and bearing in mind that is generally accepted that is easier to converge the geometrical parameters than the energetic ones, we are confident that the inclusion of a larger proportion of the correlation energy would not significantly affect the geometry of the computed complexes.

The differences between the interaction energies computed at the MP2/aug-cc-pVTZ and MP2/aug-cc-pV5Z levels of theory are much acuter. The aug-cc-pVTZ basis set consistently underestimates the MP2 interaction energies (overestimates the absolute value of the interaction energies), as compare to the MP2/aug-cc-pV5Z values (m.s.d. = -0.292 kcal/mol, m.a.e. = 0.292 kcal/mol). On the other hand, if we compare the corresponding counterpoise (CP) corrected values, CP-MP2/aug-cc-pVTZ vs. CP-MP2/aug-cc-pV5Z, the average error is greatly reduced (m.s.d. = 0.056 kcal/mol, m.a.e. = 0.056 kcal/mol), which indicates that the BSSE is mostly responsible for the interaction energy error at the MP2/aug-cc-pVTZ level of theory. It is worth noting that the average error on the interaction energies at the MP2/aug-cc-pVQZ level of theory (m.s.d. = -0.083 kcal/mol, m.a.e. = 0.083 kcal/mol) is less than a third the corresponding average error when the aug-cc-pVTZ basis set is used. Based on these trends we cannot completely discard the need a quadruple- or quintuple-ζ basis set to get a converged geometry, but as mentioned above, getting a converged geometry is an easier task than converging the energetic values, and performing geometry optimizations at the MP2/aug-cc-pVTQZ or MP2/aug-pV5Z levels of theory would be too costly considering both the size and the number of systems studied in this work.

The absolute value of the CP-correction at the MP2/aug-cc-pV5Z is in general small (m.s.d. = -0.069 kcal/mol, m.a.e. = 0.069 kcal/mol). Furthermore, the comparison of both MP2/aug-cc-pV5Z and CP-MP2/aug-cc-pV5Z against the SAPT2/aug-cc-pVTZ results, which are free of BSSE, reveals that: first, interaction energies at the CP-MP2/aug-cc-pV5Z level of theory are very similar to the SAPT2 results but systematically overestimate (underestimated the absolute value of) the interaction energy (m.s.d. = 0.043 kcal/mol, m.a.e. = 0.048 kcal/mol), and second, interaction energies at the MP2/aug-cc-pV5Z level of theory are even more similar to the SAPT2 results but systematically underestimate (overestimated the absolute value of) the interaction energy (m.s.d. = -0.025 kcal/mol, m.a.e. = 0.027 kcal/mol). These observations allow us to conclude that at MP2/aug-cc-pV5Z interaction energies are nearly or fully converged regarding the basis set. This conclusion is also supported by the tendency of the counterpoise method to overestimate the BSSE contribution for correlated methods.[28]

Let us now explore the effect of increasing the amount of correlation energy recovered on the interaction energies that are free or nearly free of BSSE. If we compare the interaction energy results at both SAPT2+3/aug-cc-pVTZ and CCSD(T)/aug-cc-pVTZ+δ(aV5Z) levels of theory to the SAPT2/aug-cc-pVTZ interaction energies, we observe that: first, SAPT2+3/aug-cc-pVTZ always increases the absolute value of the interaction energies (m.s.d. = -0.115 kcal/mol, m.a.e. = 0.115 kcal/mol), and second, CCSD(T)/aug-cc-pVTZ+□(aV5Z) also increases the absolute value of the interaction energies (m.s.d. = -0.053 kcal/mol, m.a.e. = 0.053 kcal/mol), although the differences are always smaller than for the SAPT2+3 approach. As mentioned above, we deem CCSD(T)/aug-cc-pVTZ+δ(aV5Z) as our highest computational level; the fact that SAPT2+3 also corrects the interaction energies in the same direction reinforces our trust on the CCSD(T)/aug-cc-pVTZ+δ(aV5Z) results.

Table 1. Interaction energies at several levels of theory computed by means of single-point calculation on the MP2/aug-cc-pVTZ geometries. aVXZ stands for aug-cc-pVXZ. CP indicates couterposie (CP) corrected values while nonCP indicate values without BSSE correction. All values are given in kcal/mol.

	MP2 aVTZ		MP2 aVQZ		MP2 aV5Z		SAP0+D aVTZ	SAPT2 aVTZ	SAPT2+3 aVTZ	CCSD(T) aVTZ		CCSD(T) aVTZ+δ(zV5z)
	nonCP	CP	nonCP	CP	nonCP	CP	-	-	-	nonCP	CP	nonCP
Val-Met_0a	-1.17	-0.81	-0.99	-0.85	-0.91	-0.86	-0.96	-0.90	-0.99	-1.21	-0.87	-0.95
Val-Met_1a	-1.14	-0.79	-0.96	-0.82	-0.89	-0.83	-0.93	-0.87	-0.97	-1.19	-0.85	-0.93
Val-Met_2a	-1.17	-0.81	-0.98	-0.85	-0.91	-0.86	-0.96	-0.90	-0.99	-1.21	-0.87	-0.95
Val-Met_3a	-1.14	-0.79	-0.95	-0.82	-0.89	-0.83	-0.94	-0.87	-0.97	-1.18	-0.86	-0.93
Val-Met_4a	-0.87	-0.60	-0.73	-0.62	-0.67	-0.63	-0.72	-0.67	-0.74	-0.92	-0.66	-0.72
Val-Met_5a	-0.98	-0.66	-0.81	-0.69	-0.75	-0.70	-0.80	-0.74	-0.82	-1.03	-0.73	-0.80
Val-Met_6a	-1.93	-1.35	-1.64	-1.41	-1.53	-1.43	-1.61	-1.48	-1.63	-1.93	-1.39	-1.53
Val-Met_7a	-1.36	-0.92	-1.14	-0.96	-1.05	-0.98	-1.12	-1.02	-1.14	-1.41	-0.99	-1.10
Val-Met_8a	-2.18	-1.57	-1.90	-1.65	-1.78	-1.67	-1.96	-1.72	-1.89	-2.18	-1.61	-1.77
Val-Met_0b	-1.19	-0.83	-1.01	-0.87	-0.94	-0.88	-0.98	-0.92	-1.01	-1.23	-0.89	-0.97
Val-Met_1b	-1.16	-0.81	-0.98	-0.84	-0.91	-0.85	-0.95	-0.89	-0.99	-1.20	-0.87	-0.95
Val-Met_2b	-1.18	-0.83	-1.00	-0.86	-0.93	-0.87	-0.98	-0.92	-1.01	-1.22	-0.89	-0.97
Val-Met_3b	-1.14	-0.79	-0.95	-0.82	-0.89	-0.83	-0.93	-0.87	-0.97	-1.18	-0.86	-0.93
Val-Met_4b	-0.87	-0.60	-0.73	-0.63	-0.68	-0.63	-0.72	-0.68	-0.75	-0.92	-0.67	-0.73
Val-Met_5b	-1.03	-0.71	-0.86	-0.73	-0.79	-0.74	-0.84	-0.79	-0.87	-1.08	-0.77	-0.84
Val-Met_6b	-2.75	-2.03	-2.40	-2.11	-2.27	-2.14	-2.27	-2.08	-2.39	-2.75	-2.07	-2.27
Val-Met_8b	-2.26	-1.64	-1.97	-1.71	-1.84	-1.74	-2.03	-1.80	-1.96	-2.24	-1.66	-1.83
Val-Met_0c	-1.20	-0.83	-1.00	-0.86	-0.93	-0.87	-0.97	-0.91	-1.00	-1.22	-0.88	-0.95
Val-Met_1c	-1.15	-0.80	-0.97	-0.83	-0.90	-0.84	-0.94	-0.88	-0.98	-1.19	-0.87	-0.94
Val-Met_2c	-1.19	-0.82	-1.00	-0.86	-0.92	-0.87	-0.97	-0.91	-1.00	-1.22	-0.88	-0.95
Val-Met_3c	-1.18	-0.82	-0.99	-0.86	-0.92	-0.87	-0.97	-0.91	-1.00	-1.22	-0.89	-0.96
Val-Met_4c	-0.92	-0.64	-0.77	-0.66	-0.71	-0.67	-0.75	-0.71	-0.79	-0.96	-0.67	-0.76
Val-Met_5c	-0.93	-0.63	-0.78	-0.66	-0.71	-0.67	-0.77	-0.72	-0.79	-0.96	-0.70	-0.75
Val-Met_6c	-2.19	-1.60	-1.91	-1.68	-1.80	-1.70	-2.04	-1.81	-1.97	-2.21	-1.66	-1.82
Val-Met_7c	-1.75	-1.29	-1.53	-1.34	-1.44	-1.36	-1.65	-1.45	-1.56	-1.78	-1.34	-1.47
Val-Met_8c	-2.97	-2.17	-2.59	-2.26	-2.43	-2.29	-2.57	-2.32	-2.52	-2.87	-2.12	-2.34

Finally, it is worth highlighting how remarkable well the SAPT0+D/aug-cc-pVTZ level of theory performs for these systems compare to the SAPT2+3/aug-cc-pVTZ (m.s.d. = 0.015 kcal/mol, m.a.e. = 0.041 kcal/mol) and the CCSD(T)/aug-cc-pVTZ+δ(aV5Z) (m.s.d. = -0.047 kcal/mol, m.a.e. = 0.048 kcal/mol) levels of theory. Then, SAPT0+D/aug-cc-pVTZ seems like a valid methodology for modeling larger systems that are similar in nature to the ones studied in the present work.

Now we continue our discussion on the interaction energies by focusing on the CCSD(T)/aug-cc-pVTZ+δ(aV5Z) interaction energies. For the subgroup of complexes that exhibit potential C-H···H-C contacts between the methane and both Valine's methyl groups, **Val-Met_nx** (n = 0-3; x = a, b, c), their interactions energies lie take values between -0.93 and -0.97 kcal/mol (see **Table 1**). We mentioned on the discussion of the geometries (see above) that it is very difficult to distinguish between **Val-Met_0x**, **Val-Met_1x**, **Val-Met_2x** and **Val-Met_3x**, for a given x = a, b or c (see **Figures 1-3**), being the main different observed that **Val-Met_nx** (n = 0-2; x = a, b, c) complexes appear to interact stronger with the methyl B than methyl A (see **Chart 1**) while **Val-Met_3x** (x = a, b, c) complexes appear to interact strongly with methyl A than methyl B (see **Chart 1**). Then, geometry and energy results indicate that the methane can interact in multiple fashions with both methyl groups of the Valine's sidechain at once without important energy differences (flexible, versatile and easily distorted interactions). Furthermore, the absolute value of this interaction is also remarkable, nearly 1 kcal/mol, especially considering that only involves two methyl groups and a methane. We can envision that the value associated to this type of interactions can grow quite large if the interaction of two hydrophobic segments of a protein or the interaction of a hydrophobic moiety of a ligand with a few aliphatic sidechains in a target pocket are considered; in other words, grand goals such as the accurate estimate of

protein-protein interactions, protein stabilities and target-ligand affinity may be grossly misestimated if the C-H···H-C contacts are not properly taken into account. On the other hand, based on how flexible and versatile the interactions based on these contacts are, we can expect that the specific geometries of those systems to be controlled by other interactions more critically affected by geometrical changes, such as hydrogen bonds, without much penalizing the energetic contribution from potential C-H···H-C contacts.

Let us now consider complexes **Val-Met_nx** (n = 4, 5; x = a, b, c). These complexes only form C-H···H-C contacts and the interactions involve only one of the methyl groups of the Valine. The interaction energies for these four complexes range from -0.72 to -0.84 kcal/mol (see **Table 1**), which does not represent a dramatic decrease on the absolute value of the interaction energies compare to the complexes where the methane is interacting with both methyl groups at the same time (between 0.25 and 0.09 kcal/mol stronger for the latter). Once again, this indicates how versatile and flexible these interactions are that not only allow for the formation of multiple similar complexes involving two methyl groups in the interaction, they also can disengage one of those methyl groups without paying a high penalty in terms of interaction energy.

For series a and b, the methane in complex **Val-Met_5x** interacts strongly with the corresponding methyl group (-0.80 and -0.84 kcal/mol for x = a, b respectively, see **Table 1**) than in complex **Val-Met_4x** (-0.72 and -0.73 kcal/mol for x = a, b respectively, see **Table 1**). Interestingly, the interaction energies of **Val-Met_4c** and **Val-Met_5c** are nearly identical (-0.76 and -0.75 kcal/mol respectively, see Table 1). We do not currently have an explanation for such differences.

Finally, we consider now complexes that exhibit potential C-H···H-C contacts together with other sort of interactions: **Val-Met_nx** (n = 6, 8; x = a, b, c) and **Val-Met_7x** (x = a, c). The interaction energies of this complexes are the strongest computed in the present work, ranging from -1.10 to -2.34 kcal/mol (see **Table 1**). The two strongest complexes are **Val-Met_6b** and **Val-Met_8c** whose interaction energies are -2.27 and -2.34 kcal/mol respectively (see **Table 1**). **Val-Met_6b** exhibits two C-H···H-O close contacts (2.191 and 2.212 Å, see Figure 2) that are likely to be responsible for most of the interaction energy. **Val-Met_8c** exhibits two N-H···H-C close contacts (2.435 and 2.567 Å, see **Figure 3**) and one potential C=O···H-C contact (2.861 Å, see **Figure 3**) which are responsible for the high absolute value of the interaction energy observed.

Val-Met_8a and **Val-Met_8b**, likewise **Val-Met_8c**, also exhibits two N-H···H-C close contacts (2.437 and 2.449 Å, see **Figure 1**; 2.425 and 2.446 Å, see **Figure 2**) and one potential C=O···H-C contact (2.641 Å, see **Figure 1**; 2.632 Å, see **Figure 2**), but the interactions energies are quite smaller in absolute value (-1.77 and -1.83 kcal/mol for **Val-Met_8a** and **Val-Met_8b**, respectively, see **Table1**). We hypothesis that the internal hydrogen bond between the amine and the carboxylic acid on **Val-Met_8c** may increase the polarity of the N-H bonds, reinforcing the N-H···H-C interaction.

The interaction energy of **Val-Met_6c** is remarkably large (-1.82 kcal/mol, see **Table 1**), and we again expect is related the internal hydrogen bond which may help increase the polarity of the C=O bond, resulting on a stronger C=O···H-C contact (2.593 Å, see **Figure 3**). On the other hand, that effect is also present in **Val-Met_7c**, which also forms a C=O···H-C close contact (2.516 Å, see **Figure 3**), but whose interaction energy is smaller in absolute value (-1.47 kcal/mol, see **Table 1**). This maybe explained but the smaller number of C-H···H-C contacts on **Val-Met_7c** than on **Val-Met_6c** (see Figure 3).

Val-Met_6a and **Val-Met_7a**, they both form similar H-O···H-C contacts (2.737 Å and 2.674 Å, respectively, see **Figure 1**) but the former dimer is stronger (-1.53 kcal/mol vs. -1.10 kcal/mol, see **Table 1**). We once again suspect is due to a larger number of C-H···H-C contacts on **Val-Met_6a**.

3. Decomposition of the SAPT2 interaction energies. **Table 2** includes the interaction energies at the SAPT2/aug-cc-pVTZ for the 26 complexes located on the MP2/aug-cc-pVTZ PES. **Table 2** also includes the different components of the interaction energy using two alternative approaches of constructing those terms:

I. The SAPT2 interaction energy can be divide in five components: electrostatic (E_{el}), induction (E_{ind}), dispersion (E_{disp}), exchange (E_{xc}) and a Hartree-Fock (HF) correction (δHF).[29] E_{el} includes the interaction involving unperturbed electron densities of the monomers. E_{ind} includes the contribution from terms involving the unperturbed density of one monomer interacting with virtual orbitals of the other monomer (induce dipoles). E_{disp} includes the contribution from terms involving virtual orbitals of one monomer (induced dipoles) interacting with virtual orbitals of the other monomer (induce dipoles). All these terms are calculated without satisfying the proper symmetry of the wavefunction and that symmetry requirement is imposed afterwards by using a project operator. Hence, corrections to each of the previous terms arise, which are generally group together into an E_{xc} term. The last contribution to the interaction energy (δHF) is a mix of higher order induction terms and their exchange counterparts that is obtained from a CP-corrected HF calculation.

II. It can be argued that the exchange term is sort of an artificial contribution since it would never appear if the interaction energy were computed using a wave function with the right symmetry. Hence, we decided to group the different components of the SAPT2 interaction energy in three contributions. First, E_{el+XC} that is the result of adding together E_{el} and all the exchange terms associated with the electrostatic contribution. Second, E_{ind+XC} that is the sum of all the induction terms plus their corresponding exchange counterpart contributions (it then includes δHF). Third, $E_{disp+XC}$ that is the sum of all the induction terms plus their corresponding exchange counterpart contributions. One way to see the terms is considering them the electrostatic/induction/dispersion contribution that is compatible with a solution that satisfy the proper symmetry requirements of the wave function.

We base our discussion of the nature interaction energies on that second packaging of the perturbative contributions to the interaction energy. On doing so, a very simple picture of the nature of the complexes herein considered emerges.

Table 2. Interaction energies and its components at the SAPT2/aug-cc-pVTZ level of theory computed by means of single-point calculation on the MP2/aug-cc-pVTZ geometries. Two alternative packaging of the perturbative

components of the interaction energy are provided, one to the left of the SAPT2 interaction energies, the other to the right of the SAPT2 interaction energies. All values are given in kcal/mol.

	E_{el}	E_{ind}	E_{disp}	E_{XC}	δHF	**SAPT2**	E_{el+XC}	E_{ind+XC}	$E_{disp+XC}$
Val-Met_0a	-0.49	-0.21	-1.99	1.86	-0.07	**-0.90**	1.03	-0.09	-1.84
Val-Met_1a	-0.47	-0.20	-1.93	1.80	-0.07	**-0.87**	0.99	-0.09	-1.78
Val-Met_2a	-0.48	-0.21	-1.99	1.84	-0.07	**-0.90**	1.02	-0.09	-1.83
Val-Met_3a	-0.44	-0.19	-1.94	1.78	-0.07	**-0.87**	1.00	-0.08	-1.80
Val-Met_4a	-0.32	-0.15	-1.45	1.29	-0.05	**-0.67**	0.73	-0.06	-1.34
Val-Met_5a	-0.36	-0.16	-1.57	1.39	-0.05	**-0.74**	0.76	-0.06	-1.45
Val-Met_6a	-1.21	-0.49	-3.06	3.45	-0.16	**-1.48**	1.59	-0.27	-2.79
Val-Met_7a	-0.88	-0.37	-2.15	2.49	-0.11	**-1.02**	1.11	-0.16	-1.96
Val-Met_8a	-1.75	-0.77	-3.32	4.34	-0.22	**-1.72**	1.74	-0.47	-3.00
Val-Met_0b	-0.50	-0.23	-1.99	1.87	-0.08	**-0.92**	1.03	-0.11	-1.83
Val-Met_1b	-0.48	-0.21	-1.94	1.81	-0.07	**-0.89**	0.99	-0.09	-1.79
Val-Met_2b	-0.45	-0.21	-1.96	1.77	-0.07	**-0.92**	0.99	-0.09	-1.81
Val-Met_3b	-0.43	-0.20	-1.93	1.74	-0.06	**-0.87**	0.99	-0.08	-1.78
Val-Met_4b	-0.32	-0.15	-1.46	1.29	-0.05	**-0.68**	0.73	-0.06	-1.35
Val-Met_5b	-0.38	-0.17	-1.62	1.43	-0.05	**-0.79**	0.78	-0.07	-1.50
Val-Met_6b	-1.76	-1.32	-3.48	4.81	-0.33	**-2.08**	2.14	-1.05	-3.17
Val-Met_8b	-1.80	-0.81	-3.39	4.44	-0.23	**-1.80**	1.77	-0.52	-3.06
Val-Met_0c	-0.51	-0.24	-1.98	1.91	-0.08	**-0.91**	1.04	-0.12	-1.83
Val-Met_1c	-0.44	-0.20	-1.92	1.75	-0.07	**-0.88**	0.99	-0.09	-1.77
Val-Met_2c	-0.49	-0.23	-1.99	1.88	-0.07	**-0.91**	1.03	-0.11	-1.83
Val-Met_3c	-0.48	-0.21	-1.96	1.82	-0.07	**-0.91**	1.00	-0.10	-1.81
Val-Met_4c	-0.35	-0.17	-1.47	1.33	-0.05	**-0.71**	0.73	-0.07	-1.36
Val-Met_5c	-0.35	-0.16	-1.53	1.37	-0.05	**-0.72**	0.77	-0.07	-1.42
Val-Met_6c	-1.72	-0.87	-3.27	4.29	-0.24	**-1.81**	1.76	-0.63	-2.94
Val-Met_7c	-1.20	-0.63	-2.48	3.04	-0.18	**-1.45**	1.27	-0.48	-2.24
Val-Met_8c	-1.82	-1.22	-4.39	5.34	-0.24	**-2.32**	2.38	-0.72	-3.98

For all the 26 complexes there is no stabilizing electrostatic component, the interaction energy would be strongly repulsive if the effect of induce dipoles were not included (see Table 2). This is not surprising considering that one of the monomers is methane, a neutral nonpolar molecule.

For the complexes **Val-Met_nx** (n = 0-5; x = a, b, c), that involve a neutral nonpolar molecule exclusively interacting with the nonpolar sidechain of the Valine (see **Figures 1-3**), the main and almost unique stabilizing component is the dispersion, with a nearly negligible induction contribution (see **Table 2**). For the 12 complexes exhibiting simultaneous interactions between both methyl groups and the methane, **Val-Met_nx** (n = 0-3; x = a, b, c; see **Figures 1-3**), $E_{disp+XC}$ ranges from -1.77 to -1.84 kcal/mol while E_{ind+XC} values range from -0.08 to -0.12 kcal/mol (see **Table 2**). For the six complexes where the methane exhibit contacts with only one methyl group, **Val-Met_nx** (n = 4-5; x = a, b, c; see **Figures 1-3**), $E_{disp+XC}$ ranges from -1.34 to -1.50 kcal/mol while E_{ind+XC} values range from -0.06 to -0.07 kcal/mol (see **Table 2**). What we see here reflects the fact that dispersive interactions increase as the contact surface increases (so they are larger when the methane interacts with to methyl groups at once) but the differences in interaction energy is smaller in magnitude than the observed differences in terms of the dispersion component. This is explained in terms of a smaller electrostatic repulsion (see **Table 2**) also due to a smaller contact surface (less overlapping between the electron clouds that translates into less exchange repulsion).

Finally, let us focus our attention on the complexes that exhibit C-H···H-C contacts together with interactions between the methane and polar groups of the Valine (-CO2H and -NH2). Consequently, now dipole···induce-dipole interactions are possible and then the induction contribution is larger than for the previously considered complexes: -0.16 kcal/mol for Val-Met_7a, -0.27 kcal/mol for Val-Met_6a, -0.47 kcal/mol for Val-Met_8a, -0.48 kcal/mol for Val-Met_7c, -0.52 kcal/mol for Val-Met_8b, -0.63 kcal/mol for **Val-Met_6c**, -0.72 kcal/mol for **Val-Met_8c**, and -1.05 kcal/mol for Val-Met_6b (see **Table 2**). Furthermore, the dispersion term is also boosted taking values between -1.96 and -3.98 kcal/mol (see **Table 2**). During the discussion of the geometries, we saw that those interactions between the methane and the polar groups were in some cases characterized by very short contacts, which translates into higher repulsive electrostatic

interactions (see **Table 2**). For instance, **Val-Met_6b** exhibits two C-H···H-O close contacts around 2.2 Å (see **Figure 2**) and consequently a very high electrostatic (repulsive) interaction energy component (2.14 kcal/mol, see **Table 2**). Similarly, **Val-Met_8c** exhibits two C-H···H-N close contacts around 2.4 Å (see **Figure 2**) and the highest electrostatic (repulsive) interaction energy component (2.38 kcal/mol, see **Table 2**). These increases in the electrostatic repulsion partially reduce the stability gains due to larger induction and dispersion contributions.

4. QTAIM topological analysis of the intermolecular interactions. **Figures 4-6** show the result of a topological analysis of the electron density focused on the existence of bond critical points between the methane and the different functional groups of the Valine.

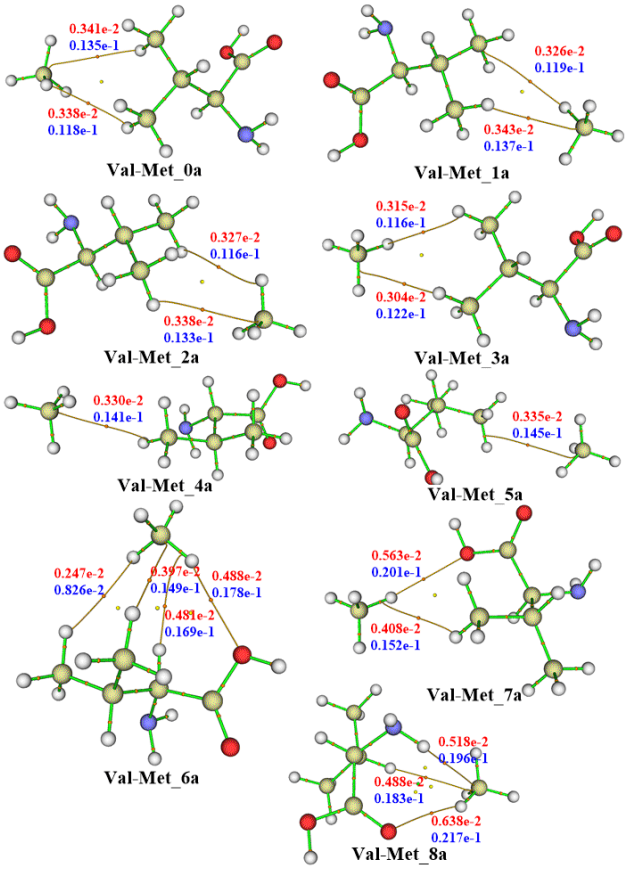

Figure 4. QTAIM topological analysis of the electron density for the complexes belonging to series a. Values of the electron density (red) and Laplacian of the electron density (blue) for BCPs linking methane and Valine are shown. All values are given in atomic units (a.u.).

The picture arising from the QTAIM analysis is quite heterogeneous in the sense that it strongly depends on the specific structure considered, instead of just the groups involved in each interaction.

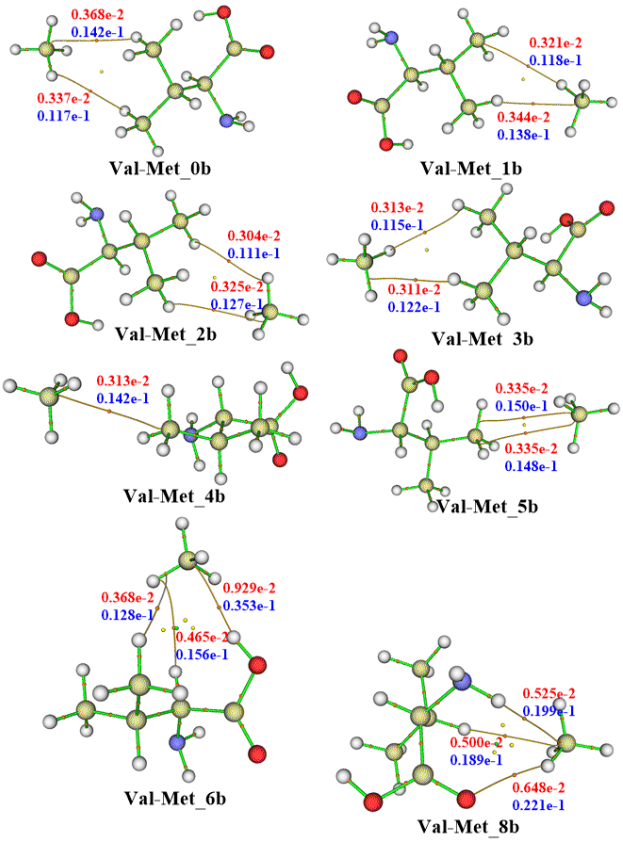

Figure 5. QTAIM topological analysis of the electron density for the complexes belonging to series b. Values of the electron density (red) and Laplacian of the electron density (blue) for BCPs linking methane and Valine are shown. All values are given in atomic units (a.u.).

For instance, let us compare **Val-Met_0a** and **Val-Met_1a**. Both structures are examples of complexes where the methane interacts with both Valine's methyl groups (see **Figure 1**). This is confirmed by the fact that there are two BCPs connecting methane and Valine on each complex, but while for **Val-Met_0a** one BCP connects two hydrogens and the other the carbon center of the methane and a hydrogen from the other methyl (see **Figure 4**), for **Val-Met_1a** one BCP connects a Valine's hydrogen with the methane's carbon and the other links a methane's hydrogen with the carbon of the other Valine's methyl group (see **Figure 4**). Furthermore, if we consider the 12 **Val-Met_nx** (n = 0-3; x = a, b, c) complexes exhibiting interaction between the methane and both Valine's methyl groups (see **Figures 1-3**), in all cases there are two BCPs (linking the methane with each of the methyl groups) but the types of "weak bonding" involved form a very diverse mix: C-H···H-C, (methane) C-H···C-H (methyl), (methyl) C-H···C-H (methane), and even a (methyl) CH's BCP···H-C (methane) (see **Figures 4-6**). We do not consider that those differences indicate any difference on the nature of the interactions for those 12 complexes. The presence of only one BCP per pair of interacting groups is likely a consequence of multiple C-H···H-C contacts composed by patches of low electron density forming two clusters, one for each methyl group. The addition of the density from these patches within each cluster may result in the presence of one single, not very meaningful maximum. The specific atoms connected by the associated BP are probably not meaningful at

all unlikely what would happen if the contacts involve large amounts of share, concentrated electron density such as with a covalent bond.

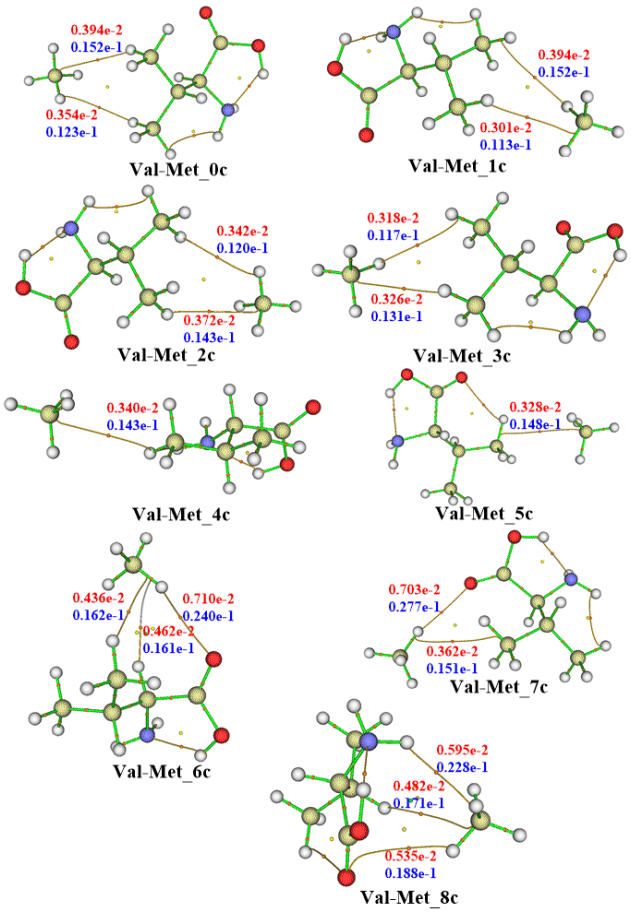

Figure 6. QTAIM topological analysis of the electron density for the complexes belonging to series c. Values of the electron density (red) and Laplacian of the electron density (blue) for BCPs linking methane and Valine are shown. All values are given in atomic units (a.u.).

It is reassuring to verify that for all the Valine's groups that appear to form contacts with the methane on the base of a simple analysis of atom-atom distances (see Figures 1-3), at least one BCP always exists between such a group and the methane, and the corresponding BPs in fact link both moieties (see **Figures 4-6**). We have seen that this is true for the 12 **Val-Met_nx** (n = 0-3; x = a, b, c) complexes (see above) and this trend still continuous when complexes involving more diverse types of contacts are considered. For instance, the three **Val-Met_8x** (x = a, b, c) complexes which were assumed to create contacts the hydrogens of the amin group, the hydrogen of the carbon β, and with the carbonyl's oxygen of the acid group, while forming no contacts with the methyl groups of the sidechain (see **Figures 1-3**); the three BCPs located on each of the complexes confirm these assumptions regarding the interactions (see **Figure 4-6**), being these three complexes the only ones lacking BCPs whose BPs linking at least one methyl groups to the methane monomer. Likewise, for complexes **Val-Met_7x** (x = a, c) (see **Figures 1-3**), a unique BCP for each Valine's group assume to form contacts with the methane is located and the corresponding BPs link that group with a critical point associated with the methane monomer (see **Figures 4-6**). One of the few exceptions happen when the three **Val-Met_6x** (x = a, b, c) are considered, based on the geometrical parameters collected on **Figures 1-3** and **Chart 1**, the methane in these complexes seems to clearly interact with carbon B but not necessarily with carbon A (see **Chart 1**). The QTAIM analysis, shows BCP bonding the methane with carbon B's methyl group, but only **Val-Met_6a** exhibits a BCP linking carbon A's methyl and the methane. It is precisely complex **Val-Met_6x** the one that exhibit the shortest C···C distance (see **Chart 1**). The presence of BCPs and BPs linking the methane to aliphatic groups supports the hypothesis that these groups are in contact due to stabilizing interactions and not just as a consequence of adopting a geometry that allows for better capturing stronger interactions such as O-H···H-C, but it is not enough to completely rule out a steric repulsion between the aliphatic groups, as other authors pointed out in the case of the planar biphenyl.[11, 13b]

Finally, let us look at the complexes which only exhibit contacts between the methane and only one of the methyl groups, Val-Met_nx (n = 4-5; x = a, b, c) (see Figures 1-3). For all the previous complexes there is only one BCP per Valine's group in contact with the methane. That is also the case for all the Val-Met_4x (x = a, b, c) and Val-Met_5x (x = a, c) (see Figures 4-6) but not for of Val-Met_5b, which interestingly has two BCPs associated to the methyl-methane interaction, both of them indicating bonding between the carbon centers (see Figure 5). This two BCPs and the corresponding ring critical point (RCP) have associated very similar values of the electron density (0.00355 a.u. for both BCPs and 0.00354 a.u. for the RCP); it is likely that this bifurcation is not stable and that a small perturbation of the system might collapse those three critical points into just one BCP. For these six complexes, the type interactions defined by the BPs depends on the specific structure considered and once again we hypothesis that is just due to a surface contact between both monomers associated with low a nearly constant values of the electron density.

It is plausible to assume that a QTAIM analysis focused on the properties of the BCPs is not the best approach to characterize these interactions involving C-H···H-C contacts since the density is going to be low and nearly evenly distributed on a large contact surface area. In spite of that, the properties of the BCPs still preserve a good predictive power as revealed by the plots of the CCSD(T)/aug-cc-pVTZ+δ(aV5Z) interaction energy versus the sum of the density at the BCPs and versus the sum of the Laplacian of the electron density at the BCPs (see **Figure 7**).

Figure 7 also includes four different linear models that can predict the interaction energy based on the sum of the values of the (Laplacian of the) electron density at the BCPs. We can use these models to estimate the contribution of the interactions involving nonpolar groups (methane-methyl and methane-carbon β) on the complexes that also engage in interactions with polar groups of the Valine. We can do so by computing the ratio between the interaction energy predicted using only the BCPs associated to nonpolar interactions and the interaction energy predicted using all the intermolecular BCPs. Using the average of the four models we estimate that the interaction of the methane with the non-polar group is responsible for 63 % (**Val-Met_6a**), 37 % (**Val-Met_7a**), 35

% (**Val-Met_8a**), 42 % (**Val-Met_6b**), 37 % (**Val-Met_8b**), 51 % (**Val-Met_6c**), 43% (**Val-Met_7c**) and 36 % (**Val-Met_8c**) of the total interaction energy of these complexes. These results indicate that ignoring the contribution of the C-H···H-C contacts may result in a gross misestimation of the interaction energy.

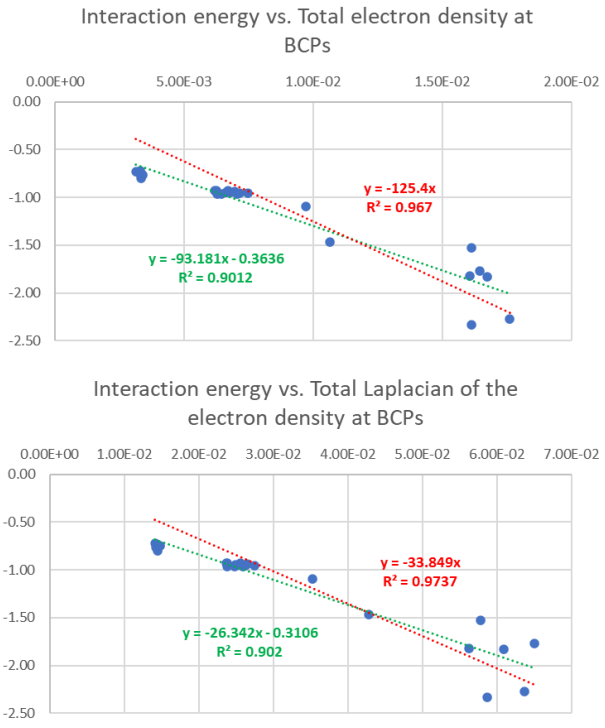

Figure 7. Scatter plots representing the CCSD(T)/aug-cc-pVTZ+δ(V5Z) interaction energies against the total electron density at the BCPs (top) and against the total Laplacian of the electron density (bottom). For each plot, two lineal models are provided, one that assumes zero bias and a second one that allows for the optimization of the y-intercept. All complexes but **Val-Met_5b** were used for the optimization of the models. Values of the electron density and Laplacian of the electron density for are given in atomic units (a.u.), while the values of the interaction energies are given in kcal/mol.

5. NCI analysis of the intermolecular interactions. Figures 7-10 show NCI plots for the 26 complexes located on the MP2/aug-cc-pVTZ PES. The strengths of this approach are complementary to the QTAIM topological analysis: they identify patches of constant reduce density gradient that can be easily associated to contacts between moieties. Highly directional interactions involving linear contacts (such as hydrogen bonds) are expected to produce tighter, smaller patches. Nondirectional interactions involving multiple atoms and broad contact surfaces are expected to produce large, spread patches. Additionally, the patches are colored based on the values of the sign(λ_2)ρ (being ρ the electron density and λ_2 the second largest eigenvalue of the diagonalized Hessian matrix of the density $\nabla^2\rho = \lambda_1 + \lambda_2 + \lambda_3$). Using a red-blue-green (RGB) scheme we get red areas when the density is being depleted (such as on a steric interaction), blue when there is an important accumulation of electron density on area (such as a strong hydrogen bond) and greenish values when there is a low accumulation of electron density (London forces, very weak hydrogen bonds).

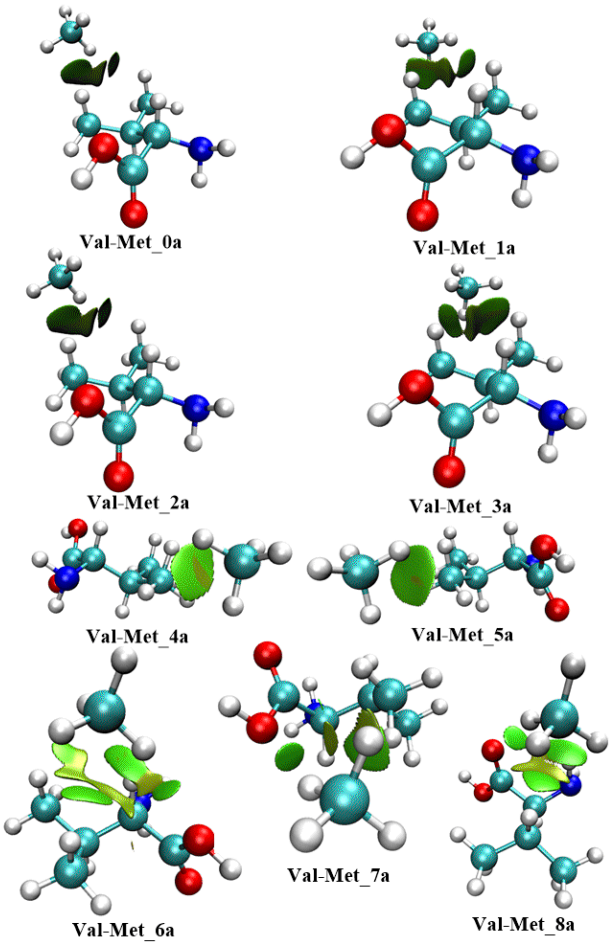

Figure 8. NCI plots for the complexes belonging to series a. Reduce gradient isosurfaces were drawn at a constant value of 0.5 a.u., and colored based on a RGB scheme according to the values of values of sign(λ_2)ρ between -0.040 and 0.020 a.u.

The NCI plots support what we have already concluded or hypothesized about the interactions in these complexes. Let us first consider the complexes **Val-Met_nx** (n = 0-3; x = a, b, c), which are expected to include only interactions of the methane with both Valine's methyl groups based on QTAIM and the analysis of the geometrical parameters (see **Figures 1-6**). A green colored patch appears between the methane and the methyl groups indicating a van der Waals interaction between these groups, although it seems to hint towards a methane-isopropyl interaction more than two methane-methyl interactions. The patch resembles the shape of an open-winged butterfly, hinting that it may be the result of three overlapping patches, one for each methane-methyl interaction (the "wings") and one located between the isopropyl's central carbon and the methane (the "body"), see **Figures 8-10**.

For complexes **Val-Met_nx** (n = 4-5; x = a, b, c). which are expected to include only interactions of the methane with one of the Valine's methyl groups, based on the QTAIM and the geometrical analyses (see **Figures 1-6**), the NCI method produces one green colored patch between the methane and the corresponding methyl group which what the weak dispersive-based interaction is formed.

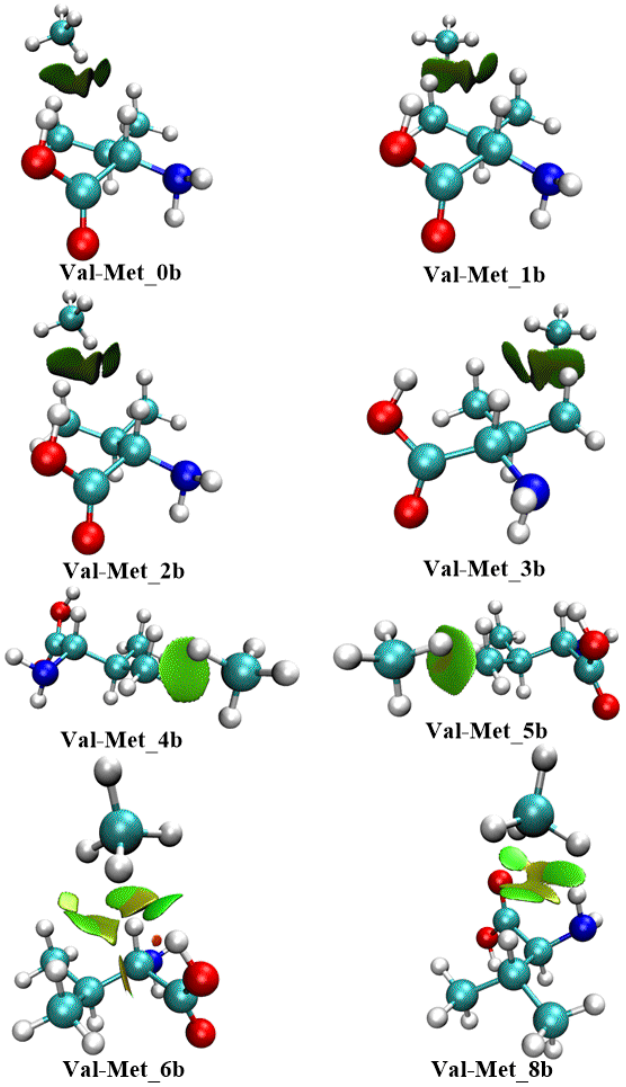

Figure 9. NCI plots for the complexes belonging to series b. Reduce gradient isosurfaces were drawn at a constant value of 0.5 a.u., and colored based on a RGB scheme according to the values of values of sign(λ_2)ρ between -0.040 and 0.020 a.u.

For the complexes **Val-Met_nx** (n = 6, 8; x = a, b, c) and **Val-Met_7x** (x = a, c), where C-H···H-C contacts coexist with interaction between the methane and Valine's polar groups (see **Figures 1-6**), green isosurfaces of reduce gradient of the density are always found between the nonpolar groups and the methane (see **Figures 8-10**), indicating that those contacts are also contributing to the stabilization of the complexes instead of representing a steric interaction penalty to pay in order to maximize the (stronger) interactions between the methane and the polar groups. Regarding the interactions between the methane and the polar groups, often appear as independent, more compact patches of green color, what indicates that despite of being expected to be stronger and despite including a no negligible induction component (not just only dispersion), their strength lies within the range of weak noncovalent interactions. This represents a good agreement with our estimate of a 35 to 63 % contribution to the interaction energy for the nonpolar-nonpolar contacts on these complexes (see above). Interestingly, for the three **Val-Met_6x** (x = a, b, c) complexes the NCI plots indicate that the methane is interacting with both Valine's methyl groups, despite Val-Met_6a being the only one that exhibits BCPs that links the methane with both groups (see Figures 4-6).

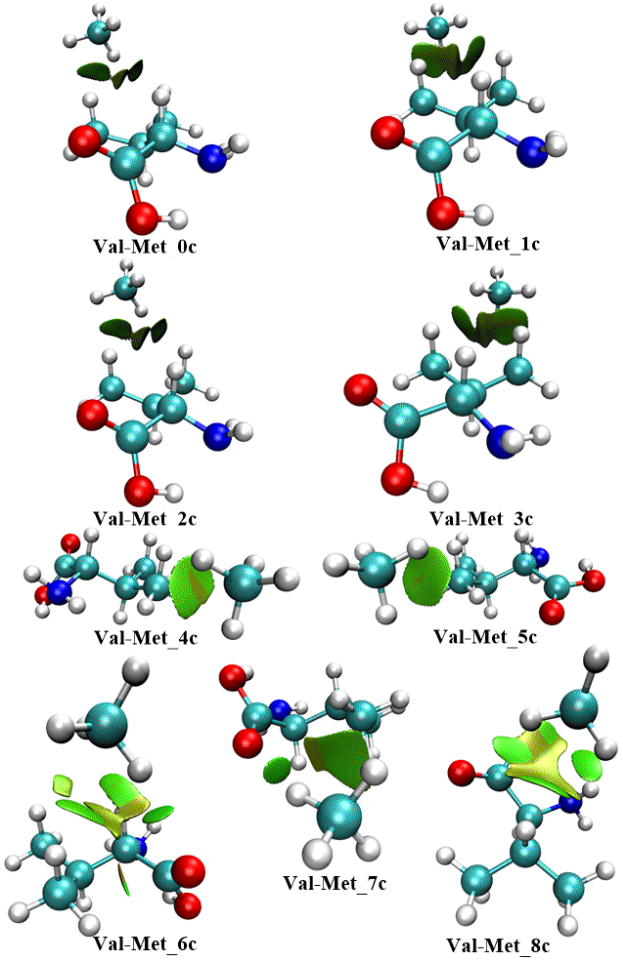

Figure 10. NCI plots for the complexes belonging to series c. Reduce gradient isosurfaces were drawn at a constant value of 0.5 a.u., and colored based on a RGB scheme according to the values of values of sign(λ_2)ρ between -0.040 and 0.020 a.u.

CONCLUSIONS

In the current study, we have located 26 Valine-methane weak complexes featuring prominent C-H···H-C contacts. For the complexes that only exhibit C-H···H-C contacts, the structures tend to maximize the number of these contacts and the interaction energies range from 0.7 to 1.0 kcal/mol, which are quite large considering that are the result of a single methane molecule interacting with one or two methyl groups. As expected, the complexes are held together by dispersion forces which must overcome a strong electrostatic repulsion between both fragments.

For the complexes that also exhibit other types of contacts, namely C-H···H-O, C-H···O and C-H···H-N, the interaction energies are larger and range from 1.1 to 2.3 kcal/mol. Consequently, the contacts between the methane and more polar and polarizable groups of the Valine, both the dispersion and the induction components make larger contributions to the interaction energy, being the dispersion still the main contribution. Our preliminary analyses of these complexes indicate

that the potential C-H···H-C contacts are still strongly contributing to the stabilization of the complexes and are not just a geometrical artifact derived from the formation of stronger interactions. This conclusion is supported by the QTAIM and NCI analyses carried out in this work.

ASSOCIATED CONTENT

(Word Style "TE_Supporting_Information"). **Supporting Information**. "This material is available free of charge via the Internet at http://pubs.acs.org."

AUTHOR INFORMATION

Corresponding Author

* ssirimulla@utep.edu.

Present Addresses

†If an author's address is different than the one given in the affiliation line, this information may be included here.

Author Contributions

The manuscript was written through contributions of all authors. / All authors have given approval to the final version of the manuscript. / ‡These authors contributed equally.

Funding Sources

This work is support from the National Science Foundation through NSF-PREM grant #DMR-1827745

Notes

Any additional relevant notes should be placed here.

ACKNOWLEDGMENT

We acknowledge the Texas Advanced Computing Center (TACC) at The University of Texas at Austin for providing HPC resources that have contributed to the research results reported within this paper. URL: http://www.tacc.utexas.edu.

ABBREVIATIONS

CCR2, CC chemokine receptor 2; CCL2, CC chemokine ligand 2; CCR5, CC chemokine receptor 5; TLC, thin layer chromatography.

REFERENCES

(1) (a) Derewenda, Z. S.; Lee, L.; Derewenda, S. U. The occurrence of C-H···O hydrogen bonds in proteins. *J. Mol. Biol.* **1995**, *252*, 248-262. (b) Torshin, I. Y.; Weber, I. T.; Harrison, R. W. Geometric criteria of hydrogen bonds in proteins and identification of 'bifurcated' hydrogen bonds. *Protein Eng.* **2002**, *15*, 359-363. (c) Escobedo, A.; Topal, B.; Kunze, M. B. A.; Aranda, J.; Chiesa, G.; Mungianu, D.; Bernardo-Seisdedos, G.; Eftekharzadeh, B.; Gairí, M.; Pierattelli, R.; Felli, I. C.; Diercks, T.; Millet, O.; García, J.; Orozco, M.; Crehuet, R.; Lindorff-Larsen, K.; Salvatella, X. Side chain to main chain hydrogen bonds stabilize a polyglutamine helix in a transcription factor. *Nat. Commun.* **2019**, *10*, 2034.

(2) (a) Hendsch, Z. S.; Tidor, B. Do salt bridges stabilize proteins? A continuum electrostatic analysis. *Protein. Sci.* **1994**, *3*, 211-226. (b) Musafia, B.; Buchner, V.; Arad, D. Complex Salt Bridges in Proteins: Statistical Analysis of Structure and Function. *J. Mol. Biol.* **1995**, *254*, 761-770. (c) Basu, S.; Mukharjee, D. Salt-bridge networks within globular and disordered proteins: characterizing trends for designable interactions. *J. Mol. Model.* **2017**, *23*, 206. (d) Ban, X.; Lahiri, P.; Dhoble, A. S.; Gu, Z.; Li, C.; Cheng, L.; Hong, Y.; Li, Z.; Kaustubh, B. Evolutionary Stability of Salt Bridges Hints Its Contribution to Stability of Proteins. *Comput. Struct. Biotechnol. J.* **2019**, *17*, 895-903.

(3) (a) Kellis Jr., J. T.; Nyberg, K.; Sali, D.; Fersht, A. R. Contribution of hydrophobic interactions to protein stability. *Nature* **1988**, *333*, 784-786. (b) Aksel, T.; Majumdar, A.; Barrick, D. The contribution of entropy, enthalpy, and hydrophobic desolvation to cooperativity in repeat-protein folding. *Structure* **2011**, *19*, 349-360. (c) Pace, C. N.; Fu, H.; Trevino, S. R.; Shirley, B. A.; Hendricks, M. M.; Limura, A.; Gajiwala, K.; Scholtz, J. M.; Grimsley, G. R. Contribution of hydrophobic interactions to protein stability. *J. Mol. Biol.* **2011**, *408*, 514-528. (d) van der Vegt, N. F. A.; Nayar, D. The Hydrophobic Effect and the Role of Cosolvents. *J. Phys. Chem. B* **2017**, *121*, 9986-9998.

(4) (a) Burley, S. K.; Petsko, G. A. Aromatic-aromatic interaction: a mechanism of protein structure stabilization. *Science* **1985**, *229*, 23-28. (b) Scheiner, S. Weak H-bonds. Comparisons of CH···O to NH···O in proteins and PH···N to direct P···N interactions. *Phys. Chem. Chem. Phys.* **2011**, *13*, 13860-13872. (c) Mohan, N.; Vijayalakshmi, K. P.; Koga, N.; Suresh, C. H. Comparison of aromatic NH···π, OH···π, and CH···π interactions of alanine using MP2, CCSD, and DFT methods. *J. Comp. Chem.* **2010**, *31*, 2874-2882. (d) Prajapati, R. S.; Sirajuddin, M.; Durani, V.; Sreeramulu, S.; Varadarajan, R. Contribution of Cation−π Interactions to Protein Stability. *Biochemistry* **2006**, *45*, 15000-15010. (e) Gromiha, M. M.; Durani, V. Distinct roles of conventional non-covalent and cation−π interactions in protein stability. *Polymer* **2005**, *46*, 983-990. (f) Chakrabarti, P.; Samanta, U. CH/pi interaction in the packing of the adenine ring in protein structures. *J. Mol. Biol.* **1995**, *251*, 9-14. (g) Brandl, M.; Weiss, M. S.; Jabs, A.; Suhnel, J.; Hilgenfeld, R. C-H...pi-interactions in proteins. *J. Mol. Biol.* **2001**, *307*, 357-377. (h) Nishio, M.; Hirota, M. CH/π interaction: Implications in organic chemistry. *Tetrahedron* **1989**, *45*, 7201-7245. (i) Umezawa, Y.; Nishio, M. CH/π interactions in the crystal structure of class I MHC antigens and their complexes with peptides. *Bioorganic. Med. Chem.* **1998**, *6*, 2507-2515. (j) Tsuzuki, S.; Honda, K.; Uchimaru, T.; Mikami, M.; Tanabe, K. The Magnitude of the CH/π Interaction between Benzene and Some Model Hydrocarbons. *J. Am. Chem. Soc.* **2000**, *122*, 3746-3753.

(5) Bader, R. F. W. *Atoms in Molecules: A Quantum Theory.*; Oxford University Press, Oxford (UK), 1990.

(6) Matta, C. F.; Hernandez-Trujillo, J.; Tang, T.-H.; Bader, R. W. F. Hydrogen–Hydrogen Bonding: A Stabilizing Interaction in Molecules and Crystals. *Chem. Eur. J.* **2003**, *9*, 1940-1951.

(7) (a) Morokuma, K. Molecular Orbital Studies of Hydrogen Bonds. III. C=O···H–O Hydrogen Bond in H2CO···H2O and H2CO···2H2O. *J. Chem. Phys.* **1971**, *55*, 1236-1244; (b) K. Morokuma, K.; Kytaura K. Energy Decomposition Analysis of Molecular Interactions. In *Chemical Applications of Atomic and Molecular Electrostatic Potentials;* Politzer, P.; Truhlar, D. G.; Springer, New York (NY), 1981; pp. 215-242. (c) Ziegler, T.; Rauk, A. On the calculation of bonding energies by the Hartree Fock Slater method. *Theor. Chem. Acta* **1977**, *46*, 1-10.

(8) Poater, J.; Sola, M.; Bickelhaupt, F. M. Hydrogen–Hydrogen Bonding in Planar Biphenyl, Predicted by Atoms-In-Molecules Theory, Does Not Exist. *Chem. Eur. J.* **2006**, *12*, 2889-2895.

(9) Bader, R. W. F. Pauli Repulsions Exist Only in the Eye of the Beholder. *Chem. Eur. J.* **2006**, *12*, 2896-2901.

(10) Poater, J.; Sola, M.; Bickelhaupt, F. M. A Model of the Chemical Bond Must Be Rooted in Quantum Mechanics, Provide Insight, and Possess Predictive Power. *Chem. Eur. J.* **2006**, *12*, 2902-2905.

(11) Hernandez-Trujillo, J.; Matta, C. F. Hydrogen–hydrogen bonding in biphenyl revisited. *Struct. Chem.* **2007**, *18*, 849-857.

(12) Palacios, L. F.; Gomez, L. Conformational changes of the electrostatic potential of biphenyl: A theoretical study. *Chem. Phys. Lett.* **2006**, *432*, 414-420.

(13) (a) Gevara-Vela, J. M.; Francisco, E.; Rocha-Rinza, T.; Pendas, A. M. Interacting Quantum Atoms—A Review. *Molecules* **2020**, *25*, 4028. (b) Popelier, P. L. A.; Maxwell, P. I.; Thacker, J. C. R.; Alkorta, I. A relative energy gradient (REG) study of the planar and

perpendicular torsional energy barriers in biphenyl. *Theor. Chem. Acc.* **2019**, *138*, 12.

(14) (a) Echeverria, J.; Aullon, G.; Danovich, D.; Shaik, S.; Alvarez, S. Dihydrogen contacts in alkanes are subtle but not faint. *Nat. Chem.* **2011**, *3*, 323-330. (b) Danovich, D.; Shaik, S.; Neese, F.; Echeverria, J.; Aullon, G.; Alvarez, S. Understanding the Nature of the CH···HC Interactions in Alkanes. *J. Chem. Theory Comput.* **2013**, *9*, 1977-1991.

(15) Alaniz, V. D.; Rocha-Rinza, T.; Cuevas, G. Assessment of hydrophobic interactions and their contributions through the analysis of the methane dimer. *J. Comput. Chem.* **2015**, *36*, 361-375.

(16) Szabo, A.; Ostlund, N. S. *Modern Quantum Chemistry*; Dover Publications, Mineola (NY), 1996.

(17) Levine, I. N. *Quantum Chemistry*, 5th edition; Prentice Hall, Upper Saddle River (NJ), 2000.

(18) Cramer, C. J. *Essentials of Computational Chemistry: Theories and Models*, 2nd Edition; John Wiley and Sons, Hoboken (NJ), 2004.

(19) Dunning, T. H. Gaussian basis sets for use in correlated molecular calculations. I. The atoms boron through neon and hydrogen. *J. Chem. Phys.* **1989**, *90*, 1007-1023.

(20) Boys, S. F.; Bernardi, F. The calculation of small molecular interactions by the differences of separate total energies. Some procedures with reduced errors. *Mol. Phys.* **1970**, *19*, 553-566.

(21) (a) Jeziorski, B.; Moszynski, R.; Szalewicz, K. Perturbation Theory Approach to Intermolecular Potential Energy Surfaces of van der Waals Complexes. *Chem. Rev.* **1994**, *94*, 1887-1930. (b) Parker, T. M.; Burns, L. A.; Parrish, R. N.; Ryno, A. G.; Sherrill, C. D. Levels of symmetry adapted perturbation theory (SAPT). I. Efficiency and performance for interaction energies. *J. Chem. Phys.* **2014**, *140*, 094106.

(22) Parrish, R. M.; Burns, L. A.; Smith, D. G. A.; Simmonett, A. C.; DePrince III, A. E.; Hohenstein, E. G.; Bozkaya, U.; Sokolov, A. Y.; Di Remigio, R.; Richard, R. M.; Gonthier, J. F.; James, A. M.; McAlexander, H. R.; Kumar, A.; Saitow, M.; Wang, X.; Pritchard, B. P.; Verma, P.; Schaefer III, H. F.; Patkowski, K.; King, R. A.; Valeev, E. F.; Evangelista, F. A.; Turney, J. M.; Crawford, T. D.; Sherrill, C. D. $P_{si}4$ 1.1: An Open-Source Electronic Structure Program Emphasizing Automation, Advanced Libraries, and Interoperability. *J. Chem. Theory Comput.* **2017**, *13*, 3185-3197.

(23) Bone, R. G. A.; Bader, R. F. W. Identifying and Analyzing Intermolecular Bonding Interactions in van der Waals Molecules. *J. Phys. Chem.* **1996**, *100*, 10892-10911.

(24) Johnson, E. R.; Keinan, S.; Mori-Sanchez, P.; Contreras-Garcia, J.; Cohen, A. J.; Yang, W. Revealing Noncovalent Interactions. *J. Am. Chem. Soc.* **2010**, *132*, 6498-6506.

(25) Lu, T.; Chen, F. Multiwfn: A multifunctional wavefunction analyzer. *J. Comput. Chem.* **2012**, *33*, 580-592.

(26) Hanwell, M. D.; Curtis, D. E.; Lonie, D. C.; Vandermeersch, T.; Zurek, E.; Hutchison, G. R. Avogadro: An advanced semantic chemical editor, visualization, and analysis platform. *J. Cheminformatics* **2012**, *4*, 17.

(27) Humphrey, W.; Dalke, A.; Schulten, K. VMD - Visual Molecular Dynamics. *J. Molec. Graphics* **1996**, *14*, 33-38.

(28) (a) Cook, D. B.; Sordo, T. L.; Sordo, J. A. On the Boys Bernardi-method to correct interaction energies calculated using M øller-Plesset perturbation theory. *J. Chem. Soc., Chem. Commun.* **1990**, 185-186. (b) Cook, D. B.; Sordo, J. A.; Sordo, T. L. Some comments on the counterpoise correction for the basis set supperposition error at the correlated level. *Int. J. Quantum Chem.* **1993**, *48*, 375-384.

(29) Bankiewicz, B.; Matczak, P.; Palusiak, M. Electron Density Characteristics in Bond Critical Point (QTAIM) versus Interaction Energy Components (SAPT): The Case of Charge-Assisted Hydrogen Bonding. *J. Phys. Chem. A* **2012**, *116*, 452-459.